# Niche expansion for phototrophic sulfur bacteria at the Proterozoic–Phanerozoic transition

Xingqian Cui[a,b,1], Xiao-Lei Liu[c], Gaozhong Shen[d], Jian Ma[a], Fatima Husain[a], Donald Rocher[e], John E. Zumberge[e], Donald A. Bryant[d,f], and Roger E. Summons[a,1]

[a]Department of Earth, Atmospheric and Planetary Sciences, Massachusetts Institute of Technology, Cambridge, MA 02139; [b]School of Oceanography, Shanghai Jiao Tong University, 200030 Shanghai, China; [c]School of Geosciences, University of Oklahoma, Norman, OK 73019; [d]Department of Biochemistry and Molecular Biology, The Pennsylvania State University, University Park, PA 16802; [e]GeoMark Research, Ltd., Houston, TX 77095; and [f]Department of Chemistry and Biochemistry, Montana State University, Bozeman, MT 59717

Edited by Donald E. Canfield, Institute of Biology and Nordic Center for Earth Evolution, University of Southern Denmark, Odense M., Denmark, and approved June 9, 2020 (received for review April 5, 2020)

**Fossilized carotenoid hydrocarbons provide a window into the physiology and biochemistry of ancient microbial phototrophic communities for which only a sparse and incomplete fossil record exists. However, accurate interpretation of carotenoid-derived biomarkers requires detailed knowledge of the carotenoid inventories of contemporary phototrophs and their physiologies. Here we report two distinct patterns of fossilized $C_{40}$ diaromatic carotenoids. Phanerozoic marine settings show distributions of diaromatic hydrocarbons dominated by isorenieratane, a biomarker derived from low-light-adapted phototrophic green sulfur bacteria. In contrast, isorenieratane is only a minor constituent within Neoproterozoic marine sediments and Phanerozoic lacustrine paleoenvironments, for which the major compounds detected are renierapurpurane and renieratane, together with some novel $C_{39}$ and $C_{38}$ carotenoid degradation products. This latter pattern can be traced to cyanobacteria as shown by analyses of cultured taxa and laboratory simulations of sedimentary diagenesis. The cyanobacterial carotenoid synechoxanthin, and its immediate biosynthetic precursors, contain thermally labile, aromatic carboxylic-acid functional groups, which upon hydrogenation and mild heating yield mixtures of products that closely resemble those found in the Proterozoic fossil record. The Neoproterozoic–Phanerozoic transition in fossil carotenoid patterns likely reflects a step change in the surface sulfur inventory that afforded opportunities for the expansion of phototropic sulfur bacteria in marine ecosystems. Furthermore, this expansion might have also coincided with a major change in physiology. One possibility is that the green sulfur bacteria developed the capacity to oxidize sulfide fully to sulfate, an innovation which would have significantly increased their capacity for photosynthetic carbon fixation.**

carotenoids | Neoproterozoic Era | phototrophic sulfur bacteria | cyanobacteria | photic zone euxinia

The transition from the Proterozoic to the Phanerozoic Eon was a pivotal time in Earth's history: The explosion in biological diversity is recorded in sedimentary rocks by a stunning array of microscopic and macroscopic fossils. During this upheaval, the biogeochemical cycles of carbon, sulfur, nitrogen, and phosphorous underwent significant reorganizations as recorded by mineral assemblages, redox-sensitive element abundances, and stable isotopic proxies that point to progressive oxygenation of the ocean–atmosphere system (1, 2). However, much of life's biological diversity is only recorded molecularly, that is, in the nucleic acids of extant organisms and in fossil molecules preserved in sediments and petroleum (3). Phototrophic bacteria, including cyanobacteria, as drivers of planetary oxygenation are particularly important as biogeochemical agents and yet their fossil record is notably obscure.

The phototrophic sulfur bacteria, ubiquitous microbes that populate illuminated aquatic environments where oxygen is absent or in trace concentrations (4), are noted for having particularly distinctive and long-lasting molecular fossils. Comprised of green sulfur bacteria (GSB; Chlorobiaceae) and purple sulfur bacteria (PSB; Chromatiaceae), these microbes serve as important sources of primary carbon fixation in environments with restricted water circulation, such as fjords, stratified seas, and saline lakes (5). They can also be productive constituents of microbial mats (6). Their presence in ancient environments is commonly recorded by distinct pigment-derived hydrocarbons preserved in sedimentary rocks and oils, typically where sediments were laid down in hypersaline lagoons, in narrow restricted seaways, and more widely during oceanic anoxic events (7–10). The oldest reported fossil carotenoids attributed to the GSB are from the Paleoproterozoic (1.65 Ga) Barney Creek Formation (BCF) of northern Australia (11).

Besides light, the other significant control on the ubiquity and productivity of GSB and PSB is sulfide availability, which, in turn, has fluctuated with the inventories of sulfur species on Earth's surface over time. Marine sulfate reservoirs apparently remained low through the Archean Eon and for most of the Proterozoic Eon (12). However, it is generally agreed that a substantial increase in marine sulfate concentrations occurred late in the Neoproterozoic coeval with a spurt in ocean

## Significance

Carotenoid pigments afford valuable clues about the chemistry and biology of both modern and ancient aquatic environments. This study reveals that fossil aromatic carotenoids—long considered biomarkers for anoxygenic, phototrophic sulfur bacteria and their physiological requirement for hydrogen sulfide and illumination—can also be biosynthesized by oxygen-producing cyanobacteria. Cyanobacterial aromatic carotenoids, which are distinct in their chemical structures and occurrence patterns, are the most commonly encountered compounds in Proterozoic marine settings as well as in lakes from more recent eras. In contrast, carotenoids diagnostic for green sulfur bacteria of the family Chlorobiaceae became both prevalent and abundant in marine paleoenvironments beginning in the Phanerozoic Eon. This expansion occurs as marine sulfate inventories increased toward the end of the Proterozoic Eon.

Author contributions: X.C. and R.E.S. designed research; X.C., X.-L.L., G.S., J.M., F.H., and R.E.S. performed research; D.R. and J.E.Z. contributed new reagents/analytic tools; X.C., X.-L.L., D.A.B., and R.E.S. analyzed data; and X.C., X.-L.L., G.S., F.H., D.A.B., and R.E.S. wrote the paper.

The authors declare no competing interest.

This article is a PNAS Direct Submission.



[1]To whom correspondence may be addressed. Email: cuixingqian@sjtu.edu.cn or rsummons@mit.edu.

This article contains supporting information online at https://www.pnas.org/lookup/suppl/doi:10.1073/pnas.2006379117/-/DCSupplemental.

First published July 9, 2020.

oxygenation (12–14). Isotopic studies suggest that the Phanerozoic oceans also experienced substantial fluctuations in sulfate levels (15–18), with estimates of concentrations that vary between ∼5 and ∼30 mM, while the modern ocean concentration stands at 28 mM. As a consequence, the spatial and secular distributions, as well as the primary productivity of phototrophic sulfur bacteria, must have been restricted in sulfide-limited Neoproterozoic seas (19). The occurrence of photic zone euxinia (PZE) during the Mesoproterozoic has so far only been reported in the BCF based on the detection of pigment-derived chemical fossils that were ascribed to phototrophic sulfur bacteria (20). While abundant evidence suggests the redox stratification of Proterozoic sea water columns (21), direct pigment evidence for PZE is confined to just a few reports (11, 22, 23).

Chemical fossils derived from pigments, exemplified by carotenoids and porphyrins, record the history of Earth's aquatic primary producers. These biomarkers, although representative of a much smaller pool of chemical diversity after diagenetic and catagenetic alteration, still preserve a highly detailed picture of precursor carotenoids and chlorophylls. The simultaneous requirement for sulfide as an electron donor and light to power anoxygenic photosynthesis (4, 24) has resulted in the aromatic carotenoids and their aryl isoprenoid derivatives being viewed as not only biomarkers for the PSB and GSB but also for situations where anoxic and sulfidic waters permanently or episodically protruded into the photic zone, that is, PZE (10, 20, 25). Aromatic carotenoids comprise 1-alkyl-2,3,4- trimethyl substituted χ-rings, as typified by okenone (V) from the PSB (26–28), and 1-alkyl-2,3,6-trimethyl-subsituted ϕ-rings as found in chlorobactene (III) and isorenieratene (XIII) from GSB (29, 30). Besides GSB and PSB, aromatic carotenoids, and the genes

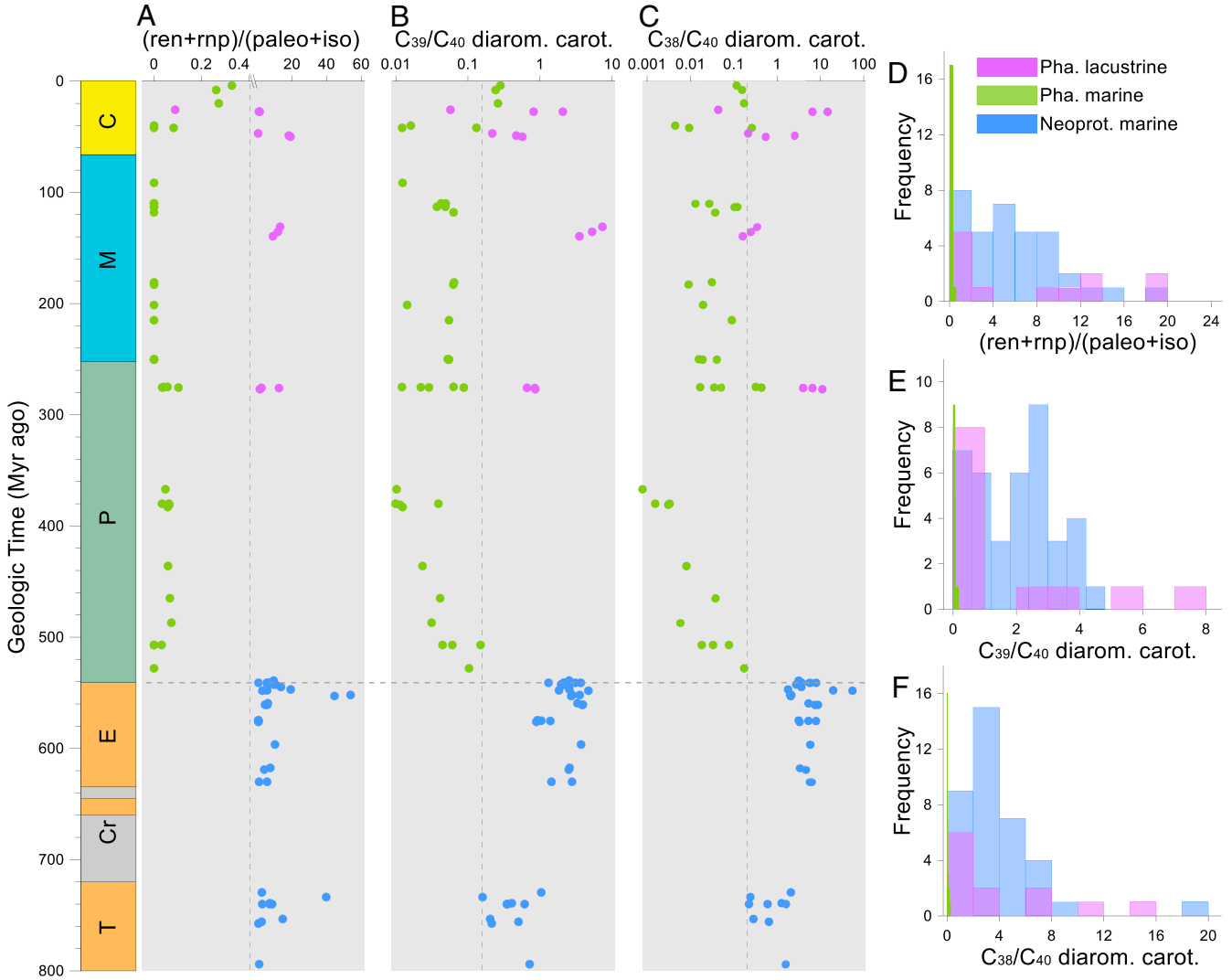


**Fig. 1.** Variation of diaromatic carotenoid-based proxies from Neoproterozoic to Cenozoic presented in geologic time and as histograms. (*A*) The ratio of (ren+rnp)/(paleo+iso) calculated based on analyses by GC-MS with dMRM acquisition of the diagnostic transition of 546→134 Da. (*B*) The sum of three $C_{39}$ diaromatic carotenoid isomers (MRM transition 532→134 Da) over the sum of all diaromatic $C_{40}$ carotenoids (MRM transition 546→134 Da). (*C*) The sum of two $C_{38}$ diaromatic carotenoid isomers (MRM transition 518→120 Da) over the sum of all $C_{40}$ diaromatic carotenoids (MRM transition 546→134 Da). The three vertical dashed lines distinguish Neoproterozoic from Phanerozoic values, and the horizontal dashed line represents the Ediacaran–Cambrian boundary. (*D–F*) Histograms of grouped Neoproterozoic marine and restricted marine (Neoprot.), Phanerozoic (Pha.) marine, and Phanerozoic (Pha.) lacustrine samples in blue, green, and purple, respectively. All Phanerozoic marine samples displayed narrow ranges, while Phanerozoic lacustrine and all Neoproterozoic samples displayed wide ranges. The legend in *D* applies to all subfigures. The abbreviations T, Cr, E, P, M, and C represent the Tonian, Cryogenian, and Ediacaran periods and Paleozoic, Mesozoic, and Cenozoic Eras, respectively.

coding for their biosynthesis, have been observed in cyanobacteria and actinobacteria (31–34).

Systematic examination of the fossil record of aromatic carotenoids (23, 35) reveals additional enigmatic compounds such as renieratane (XVIII) with one ϕ-ring and one χ-ring, renierapurpurane (XX) with two χ-rings, and β-renierapurpurpurane (XII) with one perhydro β-ring and one χ-ring. These compounds, which have structures that closely resemble precursor pigments isolated from sea sponges (36, 37), have been reported in rocks from marine and nonmarine sources that range in age from Paleoproterozoic (11, 20) to Cenozoic (35). These observations, suggesting that sponges could not be the sole or even primary source, began to make more sense once a cyanobacterial source for χ-ring carotenoids was recognized (38). Furthermore, as the biochemical and genetic basis for aromatic carotenoid biosynthesis in the GSB (29, 39, 40), PSB (27, 28), and cyanobacteria was revealed it has become increasingly clear that the environmental and geological sources for "sponge carotenoids" were likely phototrophic microbes (34).

Other understudied yet ubiquitous fossil carotenoids include β-isorenieratane (X) with one perhydro β-ring and one ϕ-ring and paleorenieratane (XVI), a diaromatic compound with one ϕ-ring and the other having a 1-alkyl-3,4,5-trimethyl substitution pattern that, to date, has not been found in any naturally occurring carotenoid (41). Biosynthetic studies, however, show that β-isorenieratene (IX) is a precursor to isorenieratene (XIII) in "brown-colored" strains of the GSB (29) and can be the predominant carotenoid in some taxa. Compound-specific carbon isotopic data for paleorenieratane (42–44) identify the GSB as the source because of the $^{13}C$ enrichment imparted by the reverse tricarboxylic acid cycle by which inorganic carbon is assimilated (45).

In the present study, we revisit the secular and environmental distribution patterns of aromatic carotenoids in the geological record, especially within the Neoproterozoic, for which reports of carotenoids are sparse. We particularly focus on the diaromatic carotenoids: isorenieratane (iso; XIV), renieratane (ren; XVIII) and renierapurpurane (rnp; XX); the bicyclic monoaromatics: β-isorenieratane (β-iso; X) and β-renierapurpurane (β-ren; XII); and two further groups of diaromatic carotenoids with 38 and 39 carbon atoms. We provide evidence for a cyanobacterial origin for the fossils renieratane, renierapurpurane (XX), and β-renierapurpurpurane (XII) and their prevalence in Proterozoic depositional settings. Finally, we present geochemical and ecological arguments for cyanobacterial diaromatic carotenoids being most prevalent in the Proterozoic with a transition to predominance of the GSB diaromatic carotenoids isorenieratane, β-isorenieratane, and paleorenieratane in Phanerozoic marine environments.

## Results

The ancient samples studied here are divided into three groups, namely, Proterozoic sediments and oils, which are likely exclusively marine in origin, and Phanerozoic samples from marine environments and Phanerozoic samples from lacustrine environments. Carotenoid biomarker distributions were measured using gas chromatography combined with precursor-product reaction-monitoring mass spectrometry with a triple quadrupole instrument (GC-QQQ-MS) as described by French et al. (23). Using this methodology, carotenoids were observed as previously reported in the BCF of the McArthur Group (11) but were undetectable in a selection of low-maturity Mesoproterozoic samples from Australia and China. However, carotenoids were widely detectable in samples of the Neoproterozoic Era and onward with significant differences in (renieratane + renierapurpurane)/(paleorenieratane + isorenieratane) [abbreviated here as (ren+rnp)/(paleo+iso)] aromatic carotenoid ratios between Neoproterozoic (0.47 to 53.8) and Phanerozoic marine samples (0 to 0.36; $P < 0.001$) and Phanerozoic marine and lacustrine samples (0.09 to 19.1; $P < 0.003$), but not between Neoproterozoic marine and Phanerozoic lacustrine samples ($P = 0.29$) (Fig. 1). Isorenieratane is commonly either the lone or the dominant diaromatic $C_{40}$ carotenoid in Phanerozoic marine samples. The single exception is the enigmatic isomer paleorenieratane (XVI) which is sometimes the most abundant diaromatic $C_{40}$ carotenoid detected in early Paleozoic samples (23, 44). Their cooccurrence and similar carbon isotopic compositions indicate that both paleorenieratane and isorenieratane represent a geochemical signature for brown-colored strains of GSB. In contrast, renieratane and renierapurpurane show their highest relative abundances in Neoproterozoic marine samples and also in Phanerozoic lacustrine samples, with the lone exception of the Oligocene Enspel Formation, an oil shale and fossil-lagerstätte deposited in a largely anoxic maar-type lake. It is noteworthy that the lowest (ren+rnp)/(paleo+iso) ratios in the Neoproterozoic sample set are found in four samples from mid-Ediacaran LMW-1 core (Officer Basin, Australia). Nevertheless, the ratios of (ren+rnp)/(paleo+iso) (0.47 to 0.62) are still significantly higher than all Phanerozoic marine samples. For most Neoproterozoic marine and Phanerozoic lacustrine samples, renierapurpurane and renieratane alternate as the most abundant $C_{40}$ diaromatic compounds (*SI Appendix*, Fig. S1), implying that a proxy based on the sum of renieratane and renierapurpurane might minimize intrabasinal biases and better capture interbasinal variations. Detailed evaluations of chlorobactane and okenane were not conducted in this study, except to note that they are both present at only trace amounts in several of the Neoproterozoic samples studied here.

A second group of prominent diaromatic carotenoids identified in this study comprise isomers with 38 and 39 carbon atoms identified on the basis of their full scan and product-ion mass spectra (*SI Appendix*, Fig. S2). The presence of β-cleavage fragment ion pairs at both 119/120 and 133/134 Da reveal that $C_{39}$ isomers are missing a single carbon atom from one of the aromatic rings, while the presence of the prominent 120-Da fragment and absence of any at 134 Da show that the $C_{38}$ isomers are missing one carbon atom from each aromatic ring of the putative $C_{40}$ precursors (*SI Appendix*, Fig. S2). The ratios of $C_{38}/C_{40}$ and $C_{39}/C_{40}$ diaromatic carotenoids display significant differences between Neoproterozoic (0.16 to 4.7 and 0 to 54.7, respectively) and Phanerozoic marine (0 to 0.38, $P < 0.001$ and 0 to 0.75, $P < 0.02$) samples. Similarly, Phanerozoic lacustrine samples (0.06 to 7.3, $P < 0.02$ and 0.05 to 14.7, $P < 0.02$) are distinct from those of marine origin. On the other hand, Proterozoic marine samples and Phanerozoic lacustrine samples resemble each other closely ($P = 0.45$ and $P = 0.26$). Variations of relative proportions of $C_{38}$ and $C_{39}$ isomers are observed between samples and are independent of ages and depositional environments, suggesting that other drivers control their relative abundances (*SI Appendix*, Figs. S1 and S3).

We also examined the carotenoids of some cultured cyanobacteria (Table 1) and conducted simulated diagenesis experiments on the carotenoids extracted from one, *Synechococcus* sp. PCC 7002. Results from these experiments (*SI Appendix*, Fig. S5) confirm that cyanobacteria, which are positive for the desaturase/transmethylase enzyme CruE and the hydroxylase/oxidase enzyme CruH, contain the diacid carotenoid synechoxanthin, its monacid and monohydroxy biosynthetic precursors, and the diaromatic hydrocarbons renierapurpurin, renieratene, and isorenieratene. Notably, the proportions of the latter were observed to differ among the cultures. While isorenieratene was always the minor isomer and mostly in traces, *Synechococcus* sp. PCC 7002 and *Leptolyngbya* sp. JSC-1 contained renierapurpurin as the major isomer, while in *Synechococcus* sp. PCC 7117 and *Synechocystis* sp. PCC 6803 renieratene was the major isomer (data not shown). In *Nostoc* sp. PCC 7120, renierapurpurin and renieratene were similar in abundance.

**Table 1. Key carotenoid biosynthesis genes in six cultured cyanobacteria and one GSB with the aromatic carotenoids identified in this study on the basis of LC-MS pigment extracts and GC-MS analyses of their hydrogenated derivatives**

| Taxon | Desaturase/ transmethylase | Hydroxylase/ oxidase | Synechoxanthin | Isorenieratene | Renieratene | Renierapurpurin |
|---|---|---|---|---|---|---|
| *Synechococcus* sp. PCC 7002 | CruE | CruH | X | X | X | X |
| *Synechococcus* sp. PCC 7117 | CruE | CruH | X | X | X | X |
| *Synechocystis* sp. PCC 6803 | CruE | CruH | X | X | X | X |
| *Nostoc* sp. PCC 7120 | CruE | CruH | X | X | X | X |
| *Synechococcus* sp. PCC 7335 | 0 | 0 | 0 | 0 | 0 | 0 |
| *Chlorobaculum limnaeum* | CrtU | 0 | 0 | X | 0 | 0 |

X = present; 0 = absent.

In the first step of simulated diagenesis, total lipid extracts of *Synechococcus* sp. PCC 7002 were subjected to mild hydrogenation in order to saturate all conjugated double bonds of the aliphatic chain of the carotenoids, thereby rendering them more thermally stable and, therefore, amenable to analysis by GC-MS (46). Because aromatic and aliphatic carboxylic acids readily decarboxylate under natural and simulated geothermal conditions (47, 48), hydrogenated total lipids of *Synechococcus* sp. PCC 7002 were heated in sealed tubes with aqueous sodium sulfide in order to promote this process in the second step (49, 50). The results of simulated diagenesis experiments showed that the (ren+rnp)/iso ratios of the *Synechococcus* sp. PCC 7002 culture fell within a narrow range between 17.4 and 24.1. In contrast, the $C_{39}/C_{40}$ and $C_{38}/C_{40}$ diaromatic carotenoid ratios increase dramatically from 0.03 and 0.00 values measured for the hydrogenated free lipids to 0.95 and 6.76 after the thermal decarboxylation experiments, respectively, with relatively more of the $C_{38}$ and $C_{39}$ products formed at higher temperatures and over longer times (*SI Appendix*, Fig. S4).

## Discussion

A number of cyanobacteria have been shown to produce carotenoids with an aromatic χ-ring (32, 38). The functional metabolite is considered to be synechoxanthin (XXV), a xanthophyll carotenoid with the structure χ,χ-caroten-18,18′-dioic acid (38). Synechoxanthin is synthesized from β-carotene (VII) via the intermediates β-renierapurpurin (XI) and renierapurpurin (XIX) through a series of desaturation/transmethylation and hydroxylation/oxidation steps catalyzed by the enzymes CruE and CruH, respectively (34). Phylogenetic profiling across a number of sequenced cyanobacteria shows that *cruE* and *cruH* genes coding for these two proteins are widely distributed across diverse taxa (32). Further, cultures of *Synechococcus* sp. PCC 7002, grown to early stationary phase, contain renierapurpurin (XIX) as a minor component (34). Accordingly, cyanobacteria are candidate sources of the fossil carotenoids β-renierapurpurane (XII) and renierapurpurane (XX). In their study of the Paleoproterozoic BCF, Brocks and Schaeffer (20) considered cyanobacteria as a potential source for renieratane, renierapurpurane, and β-renierapurpurane but rejected that possibility in favor of an origin from PSB. This was partly based upon observations reported by Behrens et al. (51), despite the demonstrated biosynthesis of β-renierapurpurin and renierapurpurin in a cultured model cyanobacterium (34) and the known potential capability for biosynthesis by other taxa from this phylum (32).

Following this logic, we document three independent lines of evidence to illustrate how cyanobacteria, in general, can potentially be significant sources of aromatic carotenoids in certain environmental settings and at specific geological time periods. First, we identified renierapurpurane along with lower amounts of renieratane and isorenieratane (Fig. 2 and *SI Appendix*, Fig. S4) in the hydrogenated lipid extracts of the cyanobacterium *Synechococcus* sp. PCC 7002. The same three aromatic carotenoids were observed when we examined four additional cyanobacteria known to have the CruE and CruH proteins (Table 1). These aromatic carotenoids were absent from *Synechococcus* sp. PCC 7335, a cyanobacterium which is devoid of both CruE and CuH. Although renieratene and isorenieratene have not previously been reported among the lipids of cyanobacteria, the results of our analyses of hydrogenated lipids from *Synechococcus* sp. PCC 7002 show that this strain is capable of de novo biosynthesis of multiple diaromatic $C_{40}$ carotenoid isomers. Their relative abundance ratios in *Synechococcus* sp. PCC 7002 remained constant after simulated geothermal heating, which confirms that methyl group migrations do not occur under the conditions employed. Overall, these results demonstrate that *Synechococcus* sp. PCC 7002 is capable of producing a suite of $C_{40}$ diaromatic carotenoid isomers with both ϕ-rings and χ-rings (*SI Appendix*, Fig. S5). They present a pattern that resembles many of the Neoproterozoic marine and Phanerozoic lacustrine samples examined in this study (Fig. 2), a pattern that also replicates recently published results for the Green River Formation (GRF) (35) and earlier work on the BCF (11).

Variations are, however, observed in the carotenoid ratios of geological samples and in cultured cyanobacteria. For example, renieratane is occasionally the dominant isomer in the GRF and can be a minor isomer in Neoproterozoic samples. In the present study, we observed that renieratene was dominant over renierapurpurin in *Synechococcus* spp. PCC 7117 and *Synechocystis* sp. PCC 6803, while in *Synechococcus* sp. PCC 7002 and *Leptolyngbya* sp. JSC-1 renierapurpurin was the dominant isomer. This suggests that the isomer distribution among diaromatic products of CruE varies from taxon to taxon or that culture conditions somehow have an impact. This contrasts to the GSB in which isorenieratene appears to be the sole product of CrtU. The diversity of taxa encoding the *cruE* gene suggests the possibility that large variations in the ratios of $C_{40}$ diaromatic carotenoid isomers might be found in natural samples without the need to implicate anoxygenic phototrophic sulfur bacteria as the sole or even primary sources (34).

Second, the bicyclic monoaromatic $C_{40}$ carotenoids β-renierapurpurane and β-isorenieratane, identified on the basis of their mass spectral characteristics and relative retention times, were identified following hydrogenation of the lipid extracts of *Synechococcus* sp. PCC 7002 (Fig. 2*A*). Unsaturated precursors are also evident in the free lipids of this organism (*SI Appendix*, Fig. S5). Given the biosynthetic pathway leading to synechoxanthin has identified β-renierapurpurin and renierapurpurin as precursors (34), detection of renierapurpurane and β-renierapurpurane in ancient samples identifies cyanobacteria as a feasible source.

A third line of evidence lies in identification of fossil hydrocarbons that are probable diagenetic products of synechoxanthin and its monocarboxylic acid precursor. The diagenetic product of the χ,χ-caroten-18,18′-dioic acid, that is, synechoxanthin (XXV), formed through hydrogenation and decarboxylation during burial in

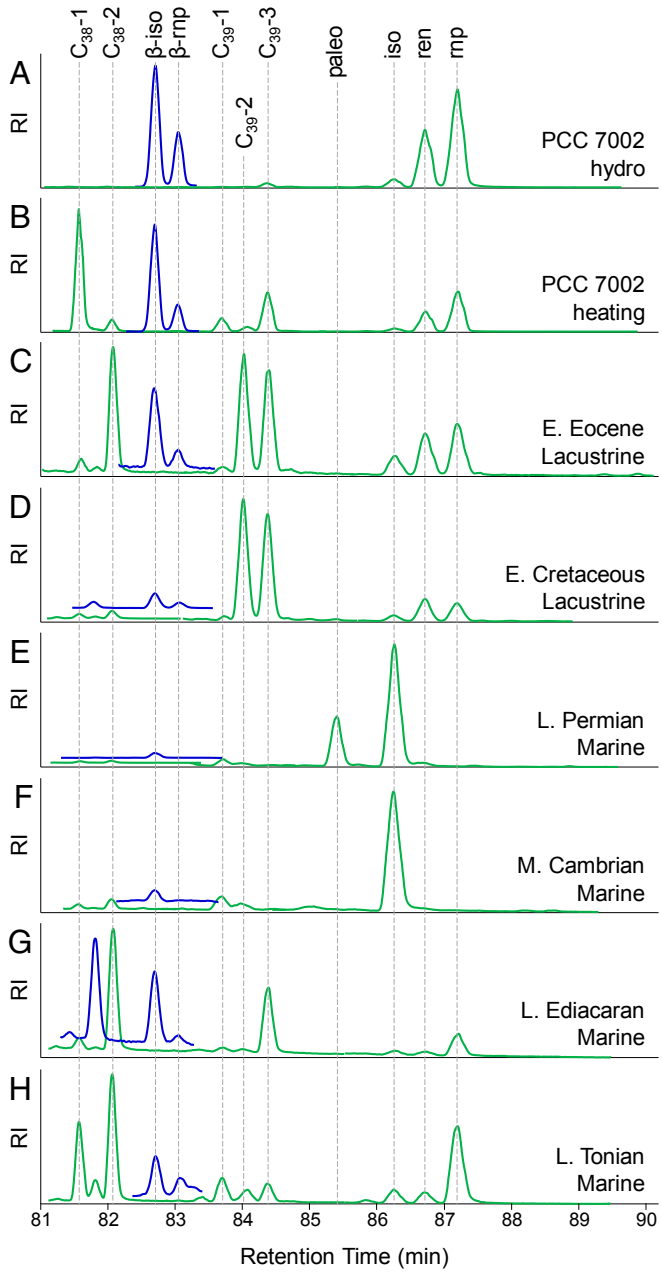


**Fig. 2.** MRM chromatograms overlain to depict distributions of $C_{38}$, $C_{39}$, and $C_{40}$ bicyclic carotenoids acquired by GC-QQQ-MS analyses of selected samples. Each group of compounds was detected using a diagnostic combination of precursor and product ions as described in the legend to Fig. 1. The nonpolar fraction of a culture of *Synechococcus* sp. PCC 7002 lipids after (*A*) mild hydrogenation alone or (*B*) hydrogenation followed by simulated geothermal heating (250 °C, 1 wk). (*C*) An early Eocene lacustrine source rock sample of the lower Green River Formation from the Uinta Basin in the United States (Coyote Wash-1, 1141 m). (*D*) An Early Cretaceous lacustrine rock from the Gabon Basin (ONEZ-1 759 m). (*E*) A Late Permian open marine sediment sample from the Peace River Basin in Canada (Apexco, 1741.3 m). Note the peak preceding isorenieratane (XIV) is paleorenieratane (XVI), and this pattern is typical for Paleozoic Era samples. (*F*) A Middle Cambrian marine shale sample of the Arthur Ck. Fm. from Georgina Basin in Australia (AGSO 5679, Owen-2). (*G*) A late Ediacaran restricted marine source rock from the South Oman Salt Basin (Birba North-1, 3901 m, A3 carbonate stringer). The first significant peak in blue is β-paleorenieratane. (*H*) A late Tonian open marine shale from the Officer Basin in Australia (Empress 1A, 629.3 m). All diaromatic carotenoids ($C_{38}$, $C_{39}$, and $C_{40}$) are shown in green, and bicyclic monoaromatic compounds [β-paleorenieratane, β-isorenieratane (X), and β-renierapurpurane (XII)] are in blue. $C_{38}$-1 and $C_{38}$-2 represent two $C_{38}$ diaromatic carotenoid isomers, and $C_{39}$-1, $C_{39}$-2, and $C_{39}$-3 are $C_{39}$ diaromatic carotenoid isomers. The form of this isomerism is not yet established. Paleo, iso, ren, rnp, β-iso, and β-rnp represent paleorenieratane (XVI), isorenieratane (XIV), renieratane (XVIII), renierapurpurane (XX), β-isorenieratane (X), and β-renierapurpurane (XII), respectively. RI denotes relative intensity.

sediments, should be a diaromatic $C_{38}$ compound with two, rather than three, methyl substituents on each ring (i.e., XXVI). Further, the monoacid biosynthetic precursor (XXII) to synechoxanthin is the logical biological precursor to the $C_{39}$ fossil counterpart (XXIII). The elevated contents of $C_{38}$ and $C_{39}$ isomers after simulated geothermal heating at higher temperatures and longer durations support their origins by decarboxylation during diagenesis. As with the $C_{40}$ diaromatic carotenoids, bicyclic monoaromatic $C_{40}$, diaromatic $C_{38}$ and $C_{39}$ carotenoids are also detected in Phanerozoic lacustrine and Neoproterozoic sediment samples. A further instance of their reported occurrence is from a Cenozoic saline lake sediment of the Qaidam Basin (52). We also note that biosynthetic gene clusters (BGCs) coding for isorenieratene synthesis have recently been identified in some *Streptomyces* species, members of the phylum Actinobacteria (53). However, because *Streptomyces* spp. are predominantly associated with decaying plant matter in soils, and these BGCs are normally silent, *Streptomyces* spp. are unlikely to be important as major sources of carotenoids in Neoproterozoic or early Paleozoic marine sediments. Although laboratory simulations imperfectly mimic natural conditions, our experiments confirm that cyanobacteria, typified by *Synechococcus* sp. PCC 7002, can be a major source of bicyclic aromatic carotenoids in modern and ancient sediments. Although previous studies found appreciable amounts of renieratene and renierapurpurin in sponges (36, 54), the fact that sponges have not been shown to be capable of de novo biosynthesis of aromatic carotenoids leads us to hypothesize that these aromatic carotenoids are biosynthetic products of cyanobacterial symbionts.

Our Proterozoic sample set, which included materials from multiple basins distributed widely in space and time, displayed a number of interesting facets. No aromatic carotenoids were detected in the Mesoproterozoic despite the samples having very high contents of organic matter, not having entered the maturation window for oil generation at which point these compounds are typically preserved. This calls into question earlier suggestions that the marine carbon cycle during these times supported significant primary productivity on the part of anoxygenic phototrophs utilizing sulfide as an electron donor (19). On the other hand, our observations are consistent with redox-sensitive trace element and iron speciation data and models that portray a seafloor that was pervasively anoxic and ferruginous (55, 56). Notably, and despite the paleogeographic spread of the sample suite, the fossil carotenoid patterns were very similar across all of the Neoproterozoic samples, which is suggestive of a relationship to ocean chemistry rather than to local features. In further support of this observation are data from some Neoproterozoic–Cambrian East Siberian crude oil samples (*SI Appendix*, Fig. S3). However, these data were not included in Fig. 1 because they are from petroleum samples rather than sediments with tight age constraints (57). To summarize, in the absence of definitive demonstrations that phototrophic sulfur bacteria or other taxa are capable of synthesizing renieratene, renierapurpurin, β-renierapurpurin, and appreciable amounts of diaromatic $C_{38}$ and $C_{39}$ derivatives, cyanobacteria are currently the only logical source of these aromatic carotenoids in Neoproterozoic seas.

A stepwise change in the pattern of sedimentary carotenoids through the Neoproterozoic–Phanerozoic transition (Fig. 1) implies a connection to developments taking place in marine biogeochemical cycles (14, 58–60) and the transitions in oceanic plankton (61, 62) that have been well documented for this time interval. The size of the marine sulfate inventory is one such

parameter that has been widely studied and provides critical context for the present study, given that it exerts a primary control on sulfide availability for anoxygenic photosynthesis. Although many reports suggest that the Neoproterozoic oceans had much lower sulfate concentrations than those of the Phanerozoic, there are great disparities in the actual estimates of the sulfate concentrations of Neoproterozoic seawater. Published ranges, constrained by fluid inclusion and evaporite compositions, include 16 to 25 mM (63), 6 to 20.5 mM (58), and 6 to 10 mM (14). Studies of paired sulfate-pyrite $\delta^{34}S$ isotope data (64), low bulk-rock concentrations of sulfur in the form of pyrite and carbonate-associated sulfate in Neoproterozoic carbonates (65), together with enriched marine sulfate $\delta^{34}S$ values spanning the Neoproterozoic–Cambrian boundary in widely separated sedimentary sections (13), provide compelling evidence for low-sulfate oceans of the time. Modeling approaches provide additional support (12, 66). One recent model connecting empirical data for S-isotopic fractionation, rates of microbial sulfate reduction (MSR), and aquatic sulfate concentrations resulted in estimates of marine sulfate concentrations of ~1 to 4 mM at the end of the Neoproterozoic rising rapidly to ~5 to 10 mM across the Ediacaran–Cambrian boundary (66).

Widespread anoxic and ferruginous conditions in low-sulfate oceans serve to throttle the availability of marine sulfide as fuel for anoxygenic photosynthesis. Evidence for this includes the occurrence of anomalous iron formations associated with platform deposits (67, 68), extensive compilations of iron speciation data (21, 69), and the overall chemistry of marine cements (70–72). Under ferruginous conditions, a high proportion of sulfide resulting from MSR in ocean margin settings would be sequestered as pyrite and rendered unavailable as an electron donor for GSB and PSB. This would also have the dual effect of hindering carotenoid preservation, because sulfide is also an essential chemical reductant for the sequestering of otherwise fragile carbon skeletons into organosulfur macromolecules (73, 74). Thus, sulfide-powered photosynthesis by GSB and PSB would be diminished in open marine environments of the Neoproterozoic when it would have been confined to restricted settings where localized accumulations of sulfate permitted a vigorous sulfur cycle to become established. An apparent and striking stepwise change in the relative abundances of isorenieratane and paleorenieratane, carotenoids of the brown-colored strains of GSB across the Ediacaran–Cambrian transition, coincides with the modeled sharp rise in marine sulfate concentrations (66).

Although modern GSB preferentially utilize sulfide as the electron donor for photosynthetic carbon fixation, and oxidize it fully to sulfate, other physiologies are observed across the phylum Chlorobi. *Chloroherpeton thalassium*, for example, can apparently only oxidize sulfide to the level of polysulfide/sulfur (75). A few GSB, for example, *Chlorobium ferrooxidans*, can also photooxidize ferrous iron, acetate, and hydrogen, but most GSB do not seem to utilize hydrogen as a preferred source of electrons for photosynthesis (76). Evidence of photoferrotrophy has been reported in a natural setting, although it seems to be slow relative to sulfide oxidation in the same place (77). These instances suggest that the ancestors of the modern members of the phylum Chlorobi, and especially the family Chlorobiaceae, differed physiologically and genomically. One key area of divergence concerns their sulfur oxidation metabolisms including the ability to oxidize sulfide completely to sulfate (78) and providing six additional electrons compared to sulfide oxidation to $S_0$. Acquisition of such a capability may have been relatively recent, geologically speaking, and would have conferred significant energetic advantages. The Paleozoic niche expansion of Chlorobiaceae, therefore, may have signaled not only increased availability of sulfide in stable anoxic environments but also coeval acquisition of advantageous physiology such as the ability to oxidize sulfide completely to sulfate.

Aromatic carotenoids, and particularly the presence of isorenieratane, have ubiquitously been applied as biomarkers for PZE. The carotenoid distribution patterns presented here, in which there are substantial amounts of renieratane and renierapurpurane and only traces of isorenieratane, are not representative of environments with PZE. Instead, they are likely indicative of seas with significant cyanobacterial primary productivity. When considered together with $C_{38}$ and $C_{39}$ diaromatic carotenoids, these distributions of aromatic carotenoids also provide a robust way to discriminate between low-sulfate lacustrine environments and marine counterparts in the Phanerozoic Eon. One cautionary note is that the $C_{38}$ and $C_{39}$ diagenetic products can be trace constituents in very immature samples (e.g., Enspel Shale) in which the decarboxylation of organic acids is minimal. Isorenieratane can only serve as an indicator for PZE in cases when it is the sole or dominant diaromatic $C_{40}$ carotenoid and/or is accompanied by detection of chlorobactane and okenane. Additionally, although β-isorenieratene can be synthesized by phototrophic GSB and some Actinobacteria (33) its detection in cyanobacteria excludes a unique association with GSB among phototrophs (51). Further work is needed to reexamine patterns of aromatic carotenoids in the rock record and carefully expand their application to paleoenvironment reconstruction.

## Materials and Methods

**Strains and Growth Conditions.** Cyanobacterial strains were selected for this study on the basis of the presence or absence of the *cruE* gene, encoding the β-carotene desaturase/methyltransferase, in their genomes. *Synechococcus* sp. PCC 7002, used for most of the experiments described here, is a unicellular, euryhaline cyanobacterium (79) that has been used to study the biosynthesis of synechoxanthin (34). Cells were grown in medium $A^+$, that is, medium A supplemented with $NaNO_3$ (1 $g{\cdot}L^{-1}$), and vitamin $B_{12}$ (10 $\mu g{\cdot}mL^{-1}$, final concentration) (80). Liquid cultures were grown at 38 °C under cool-white fluorescent illumination at an irradiance of 250 μmol photons$\cdot m^{-2}\cdot s^{-1}$ and were sparged with air supplemented with 1% (vol/vol) $CO_2$. Details of additional cyanobacterial cultures are provided in *SI Appendix*.

**Geological Samples and Methods.** A total number of 87 geological samples, including 39 Neoproterozoic marine, 36 Phanerozoic marine, and 12 Phanerozoic lacustrine rocks and crude oils, were measured in this study. Most samples were from cores, cuttings, and some outcrops and were complemented by crude oil samples where the age and origin were not in any doubt. Geographic locations, depositional environments, and age constraints are detailed in *SI Appendix*, Table S1. Briefly, Neoproterozoic samples, including Tonian and Ediacaran ages, originated from the Officer Basin, South Oman Salt Basin, Grand Canyon, and Bikaner-Nagaur Basin. These samples were deposited in either restricted basins or shallow shelves. Neoproterozoic–Cambrian age crude oils from eastern Siberia were excluded from Fig. 1. Phanerozoic marine samples originated from a variety of sedimentary environments, including restricted marine, open shelf, and distal shales while the lacustrine samples comprised material from well-established continental settings of Paleozoic, Mesozoic, and Cenozoic ages.

To avoid or mitigate contamination, rock cores and outcrops had external surfaces removed by sawing (81). Organic-lean Neoproterozoic samples were processed subsequently following the microablation technique (82). The slurry after microablation and residual clean rock pieces were denoted as "exterior" and "interior." After breaking into small pieces, each rock sample was ground in a stainless-steel puck mill which was cleaned between samples with deionized water, combusted sand, methanol (MeOH), and dichloromethane (DCM), sequentially. The powdered rocks were extracted using 100% DCM to avoid the potential loss of low-molecular-weight compounds through the evaporation of MeOH. Solvent extraction was carried out either on an accelerated solvent extractor or using the ultrasonic extraction method, followed by concentration on a TurboVap (83). Sediment extracts were separated into nonpolar and polar fractions by column chromatography on silica gel (*SI Appendix*).

**Lipid Extraction, Hydrogenation, and Simulated Diagenesis.** Harvested culture cells, upon freeze-drying, were transferred into glass centrifuge tubes and extracted with DCM:MeOH (9:1, vol:vol) using sonication and centrifugation (*SI Appendix*). After concentration, an aliquot of extracted lipids together with 5 mL of hexane, a catalytical amount of platinum oxide (Adam's

catalyst), and a magnetic stirring bar were placed in a 20-mL vial and were subjected to catalytic hydrogenation under a gentle stream of hydrogen gas for ~30 min (*SI Appendix*). Subsequently, aliquots of hydrogenated lipids, 20 to 50 μL Millipore-cleaned water, and 5 mg of sodium sulfide were placed in evacuated Pyrex tubes and heated at temperatures that ranged from 100 °C to 250 °C and for time periods of 1 d to 6 wk.

**Instrument Measurements, Compound Identification, and Quality Control.** Carotenoid analysis by liquid chromatography–mass spectrometry (LC-MS) was performed on an Agilent 1290 series ultrahigh-performance LC system coupled to an Agilent 6530 quadrupole time-of-flight mass spectrometer through an Agilent jet stream dual electrospray ionization interface. Compound separation was achieved with a reverse phase gradient and an Agilent ZORBAX SB-C18 (1.8 μm, 2.1 × 100 mm) column (*SI Appendix*, Fig. S5). Molecular structures were identified based on accurate masses of the molecular species and $MS^2$ spectra (*SI Appendix*, Fig. S6).

The nonpolar fractions of culture extracts after hydrogenation and simulated diagenesis, and from sediment and crude oils, were measured on an Agilent 7890B gas chromatograph coupled to a 7010A triple quadrupole mass spectrometer (GC-QQQ-MS) under dynamic multiple-reaction monitoring (dMRM) mode or on an Agilent mass-selective detector GC-MS system under full scan mode (*SI Appendix*). In each case, an Agilent DB-5MS column was installed with the inlet; oven and MS parameters described in detail in *SI Appendix*. Identification of bicyclic monoaromatic and diaromatic $C_{40}$ carotenoids were based on full scan spectra, product ion spectra, comparison with rock standards, authentic standards, and previously reported chromatograms (11, 20, 23, 35, 42, 52, 84) as detailed in *SI Appendix*. Diaromatic $C_{38}$ and $C_{39}$ carotenoid isomers were identified by their full scan spectra, product ion spectra, and comparisons with previous publications (42, 52, 84), although determining the precise nature of the isomerism was beyond the scope of this study. Carotenoid chromatograms for individual samples will be made available by the corresponding authors upon request.

Biomarker syngeneity was assessed on the basis of the known secular and environmental distributions of sterane triterpane and tricyclic terpane hydrocarbons and the fact that many of the samples had been previously analyzed for these components. Organic-lean Neoproterozoic samples were evaluated by comparison of exterior and interior layers after microablation with data discarded if suspicious or inappropriate biomarker ratios were observed (82).

**Data Availability.** All data pertaining to this study can be found in *SI Appendix*, Tables S1–S4.

**ACKNOWLEDGMENTS.** Financial support at the Massachusetts Institute of Technology (MIT) was provided by the Simons Foundation Collaboration on the Origins of Life and an MIT Energy Initiative project funded by Shell. Studies in the laboratory of D.A.B. were supported by grants DE-FG02-94ER20137 from the Photosynthetic Systems Program, Division of Chemical Sciences, Geosciences, and Biosciences, Office of Basic Energy Sciences of the US Department of Energy and from the NSF (MCB-1613022). We thank Dr. J. L. Thweatt for providing a chlorosome sample from *Cba. limnaeum*. We acknowledge the Geological Survey of South Australia, Geological Survey of Western Australia, Petroleum Development Oman, and Ocean Drilling Program for sample access. X.C. and R.E.S. also thank Drs. Alan Rooney, Calum Fox, Jessica Whiteside, Katherine Freeman, Gareth Izon, and Chris Boreham for sharing samples. X.C. is grateful for discussion with Dr. Gareth Izon at MIT.

1. T. W. Lyons, C. T. Reinhard, N. J. Planavsky, The rise of oxygen in Earth's early ocean and atmosphere. *Nature* **506**, 307–315 (2014).
2. H. D. Holland, The oxygenation of the atmosphere and oceans. *Philos. Trans. R. Soc. Lond. B Biol. Sci.* **361**, 903–915 (2006).
3. D. E. G. Briggs, R. E. Summons, Ancient biomolecules: Their origins, fossilization, and role in revealing the history of life. *BioEssays* **36**, 482–490 (2014).
4. N. Pfennig, Phototrophic green and purple bacteria: A comparative, systematic survey. *Annu. Rev. Microbiol.* **31**, 275–290 (1977).
5. J. Overmann, "Ecology of phototrophic sulfur bacteria" in *Sulfur Metabolism in Phototrophic Organisms*, R. Hell, D. B. Knaff, T. Leustek, Eds. (Springer, 2008), pp. 375–396.
6. H. van Gemerden, J. Mas, "Ecology of phototrophic sulfur bacteria" in *Anoxygenic Photosynthetic Bacteria*, R. E. Blankenship, R. E. Madigan, M. T. Bauer, Eds. (Springer, 1995), pp. 49–85.
7. R. D. Pancost, N. Crawford, J. R. Maxwell, Molecular evidence for basin-scale photic zone euxinia in the Permian Zechstein Sea. *Chem. Geol.* **188**, 217–227 (2002).
8. A. H. Kasprak *et al.*, Episodic photic zone euxinia in the northeastern Panthalassic Ocean during the end-Triassic extinction. *Geology* **43**, 307–310 (2015).
9. Y. van Breugel, M. Baas, S. Schouten, E. Mattioli, J. S. Sinninghe Damsté, Isorenieratane record in black shales from the Paris Basin, France: Constraints on recycling of respired CO2 as a mechanism for negative carbon isotope shifts during the Toarcian oceanic anoxic event. *Paleoceanography* **21**, PA4220 (2006).
10. J. S. Sinninghe Damsté, J. Köster, A euxinic southern North Atlantic Ocean during the Cenomanian/Turonian oceanic anoxic event. *Earth Planet. Sci. Lett.* **158**, 165–173 (1998).
11. J. J. Brocks *et al.*, Biomarker evidence for green and purple sulphur bacteria in a stratified Palaeoproterozoic sea. *Nature* **437**, 866–870 (2005).
12. D. E. Canfield, The evolution of the Earth surface sulfur reservoir. *Am. J. Sci.* **304**, 839–861 (2004).
13. G. P. Halverson, M. T. Hurtgen, Ediacaran growth of the marine sulfate reservoir. *Earth Planet. Sci. Lett.* **263**, 32–44 (2007).
14. C. L. Blättler, K. D. Bergmann, L. C. Kah, I. Gómez-Pérez, J. A. Higgins, Constraints on Meso- to Neoproterozoic seawater from ancient evaporite deposits. *Earth Planet. Sci. Lett.* **532**, 115951 (2020).
15. S. H. Bottrell, R. J. Newton, Reconstruction of changes in global sulfur cycling from marine sulfate isotopes. *Earth Sci. Rev.* **75**, 59–83 (2006).
16. B. C. Gill, T. W. Lyons, M. R. Saltzman, Parallel, high-resolution carbon and sulfur isotope records of the evolving Paleozoic marine sulfur reservoir. *Palaeogeogr. Palaeoclimatol. Palaeoecol.* **256**, 156–173 (2007).
17. I. Halevy, S. E. Peters, W. W. Fischer, Sulfate burial constraints on the Phanerozoic sulfur cycle. *Science* **337**, 331–334 (2012).
18. J. Horita, H. Zimmermann, H. D. Holland, Chemical evolution of seawater during the Phanerozoic: Implications from the record of marine evaporites. *Geochim. Cosmochim. Acta* **66**, 3733–3756 (2002).
19. D. T. Johnston, F. Wolfe-Simon, A. Pearson, A. H. Knoll, Anoxygenic photosynthesis modulated Proterozoic oxygen and sustained Earth's middle age. *Proc. Natl. Acad. Sci. U.S.A.* **106**, 16925–16929 (2009).
20. J. J. Brocks, P. Schaeffer, Okenane, a biomarker for purple sulfur bacteria (Chromatiaceae), and other new carotenoid derivatives from the 1640 Ma Barney Creek Formation. *Geochim. Cosmochim. Acta* **72**, 1396–1414 (2008).
21. C. Li *et al.*, A stratified redox model for the Ediacaran ocean. *Science* **328**, 80–83 (2010).
22. N. Gueneli *et al.*, 1.1-billion-year-old porphyrins establish a marine ecosystem dominated by bacterial primary producers. *Proc. Natl. Acad. Sci. U.S.A.* **115**, E6978–E6986 (2018).
23. K. L. French, D. Rocher, J. E. Zumberge, R. E. Summons, Assessing the distribution of sedimentary C40 carotenoids through time. *Geobiology* **13**, 139–151 (2015).
24. R. E. Blankenship, M. T. Madigan, C. E. Bauer, *Anoxygenic Photosynthetic Bacteria*, (Springer, 2006), Vol. 2.
25. R. E. Summons, T. G. Powell, *Chlorobiaceae* in Paleozoic seas revealed by biological markers, isotopes and geology. *Nature* **319**, 763–765 (1986).
26. P. Caumette, K. Schmidt, H. Biebl, N. Pfennig, Characterization of a Thiocapsa strain containing okenone as major carotenoid. *Syst. Appl. Microbiol.* **6**, 132–136 (1985).
27. K. Vogl, D. A. Bryant, Biosynthesis of the biomarker okenone: χ-ring formation. *Geobiology* **10**, 205–215 (2012).
28. K. Vogl, D. A. Bryant, Elucidation of the biosynthetic pathway for Okenone in Thiodictyon sp. CAD16 leads to the discovery of two novel carotene ketolases. *J. Biol. Chem.* **286**, 38521–38532 (2011).
29. J. A. Maresca, S. P. Romberger, D. A. Bryant, Isorenieratene biosynthesis in green sulfur bacteria requires the cooperative actions of two carotenoid cyclases. *J. Bacteriol.* **190**, 6384–6391 (2008).
30. S. Liaaen-Jensen, A. G. Andrewes, Microbial carotenoids. *Annu. Rev. Microbiol.* **26**, 225–248 (1972).
31. J. L. Klassen, Phylogenetic and evolutionary patterns in microbial carotenoid biosynthesis are revealed by comparative genomics. *PLoS One* **5**, e11257 (2010).
32. J. A. Maresca, J. E. Graham, D. A. Bryant, The biochemical basis for structural diversity in the carotenoids of chlorophototrophic bacteria. *Photosynth. Res.* **97**, 121–140 (2008).
33. H. Krügel, P. Krubasik, K. Weber, H. P. Saluz, G. Sandmann, Functional analysis of genes from Streptomyces griseus involved in the synthesis of isorenieratene, a carotenoid with aromatic end groups, revealed a novel type of carotenoid desaturase. *Biochim. Biophys. Acta* **1439**, 57–64 (1999).
34. J. E. Graham, D. A. Bryant, The biosynthetic pathway for synechoxanthin, an aromatic carotenoid synthesized by the euryhaline, unicellular cyanobacterium Synechococcus sp. strain PCC 7002. *J. Bacteriol.* **190**, 7966–7974 (2008).
35. K. L. French, J. E. Birdwell, V. Berg, Biomarker similarities between the saline lacustrine Eocene Green River and the Paleoproterozoic Barney Creek Formations. *Geochim. Cosmochim. Acta* **274**, 228–245 (2020).
36. M. Yamaguchi, Renieratene, a new carotenoid containing benzene rings, isolated from a sea sponge. *Bull. Chem. Soc. Jpn.* **31**, 739–742 (1958).
37. S. Liaaen-Jensen, B. Renstrøm, T. Ramdahl, M. Hallenstvet, P. Bergquist, Carotenoids of marine sponges. *Biochem. Syst. Ecol.* **10**, 167–174 (1982).
38. J. E. Graham, J. T. J. Lecomte, D. A. Bryant, Synechoxanthin, an aromatic C40 xanthophyll that is a major carotenoid in the cyanobacterium Synechococcus sp. PCC 7002. *J. Nat. Prod.* **71**, 1647–1650 (2008).
39. N.-U. Frigaard, D. A. Bryant, Seeing green bacteria in a new light: Genomics-enabled studies of the photosynthetic apparatus in green sulfur bacteria and filamentous anoxygenic phototrophic bacteria. *Arch. Microbiol.* **182**, 265–276 (2004).
40. J. A. Maresca, J. E. Graham, M. Wu, J. A. Eisen, D. A. Bryant, Identification of a fourth family of lycopene cyclases in photosynthetic bacteria. *Proc. Natl. Acad. Sci. U.S.A.* **104**, 11784–11789 (2007).

41. W. A. Hartgers, J. S. S. Damsté, M. P. Koopmans, J. W. de Leeuw, Sedimentary evidence for a diaromatic carotenoid with an unprecedented aromatic substitution pattern. *J. Chem. Soc. Chem. Commun.*, 1715–1716 (1993).
42. M. P. Koopmans *et al*., Diagenetic and catagenetic products of isorenieratene: Molecular indicators for photic zone anoxia. *Geochim. Cosmochim. Acta* **60**, 4467–4496 (1996).
43. W. A. Hartgers *et al*., A molecular and carbon isotopic study towards the origin and diagenetic fate of diaromatic carotenoids. *Org. Geochem.* **22**, 703–725 (1994).
44. G. T. Connock, T. X. Nguyen, R. P. Philp, The development and extent of photic-zone euxinia concomitant with Woodford Shale deposition. *AAPG Bull.* **102**, 959–986 (2018).
45. G. Fuchs, Alternative pathways of carbon dioxide fixation: Insights into the early evolution of life? *Annu. Rev. Microbiol.* **65**, 631–658 (2011).
46. P. Schaeffer, P. Adam, P. Wehrung, P. Albrecht, Novel aromatic carotenoid derivatives from sulfur photosynthetic bacteria in sediments. *Tetrahedron Lett.* **38**, 8413–8416 (1997).
47. B. Bennett, G. Abbott, A natural pyrolysis experiment–hopanes from hopanoic acids? *Org. Geochem.* **30**, 1509–1516 (1999).
48. J. Santrock, J. M. Hayes, Pyrolytic decarboxylation of aromatic acids as a means of isotopic analysis. *Anal. Chem.* **57**, 1441–1443 (1985).
49. B. R. Brown, The mechanism of thermal decarboxylation. *Q. Rev. Chem. Soc.* **5**, 131–146 (1951).
50. C. R. Glein, I. R. Gould, E. D. Lorance, H. E. Hartnett, E. L. Shock, Mechanisms of decarboxylation of phenylacetic acids and their sodium salts in water at high temperature and pressure. *Geochim. Cosmochim. Acta* **269**, 597–621 (2020).
51. A. Behrens, P. Schaeffer, S. Bernasconi, P. Albrecht, Mono- and bicyclic squalene derivatives as potential proxies for anaerobic photosynthesis in lacustrine sulfur-rich sediments. *Geochim. Cosmochim. Acta* **64**, 3327–3336 (2000).
52. C. Zhang, Y. Zhang, C. Cai, Aromatic isoprenoids from the 25–65 Ma saline lacustrine formations in the western Qaidam Basin, NW China. *Org. Geochem.* **42**, 851–855 (2011).
53. A. Becerril *et al*., Uncovering production of specialized metabolites by Streptomyces argillaceus: Activation of cryptic biosynthesis gene clusters using nutritional and genetic approaches. *PLoS One* **13**, e0198145 (2018).
54. M. Yamaguchi, On carotenoids of a sponge "Reniera japonica". *Bull. Chem. Soc. Jpn.* **30**, 111–114 (1957).
55. N. J. Planavsky *et al*., Widespread iron-rich conditions in the mid-Proterozoic ocean. *Nature* **477**, 448–451 (2011).
56. C. T. Reinhard *et al*., Proterozoic ocean redox and biogeochemical stasis. *Proc. Natl. Acad. Sci. U.S.A.* **110**, 5357–5362 (2013).
57. A. E. Kelly, G. D. Love, J. E. Zumberge, R. E. Summons, Hydrocarbon biomarkers of neoproterozoic to lower Cambrian oils from eastern Siberia. *Org. Geochem.* **42**, 640–654 (2011).
58. L. C. Kah, T. W. Lyons, T. D. Frank, Low marine sulphate and protracted oxygenation of the Proterozoic biosphere. *Nature* **431**, 834–838 (2004).
59. C. T. Reinhard *et al*., Evolution of the global phosphorus cycle. *Nature* **541**, 386–389 (2017).
60. D. E. Canfield, A. Teske, Late Proterozoic rise in atmospheric oxygen concentration inferred from phylogenetic and sulphur-isotope studies. *Nature* **382**, 127–132 (1996).
61. J. A. Zumberge, D. Rocher, G. D. Love, Free and kerogen-bound biomarkers from late Tonian sedimentary rocks record abundant eukaryotes in mid-Neoproterozoic marine communities. *Geobiology* **18**, 326–347 (2020).
62. J. J. Brocks *et al*., The rise of algae in Cryogenian oceans and the emergence of animals. *Nature* **548**, 578–581 (2017).
63. S. T. Brennan, T. K. Lowenstein, J. Horita, Seawater chemistry and the advent of biocalcification. *Geology* **32**, 473–476 (2004).
64. D. A. Fike, J. P. Grotzinger, A paired sulfate–pyrite δ34S approach to understanding the evolution of the Ediacaran–Cambrian sulfur cycle. *Geochim. Cosmochim. Acta* **72**, 2636–2648 (2008).
65. J. B. Ries, D. A. Fike, L. M. Pratt, T. W. Lyons, J. P. Grotzinger, Superheavy pyrite (δ34Spyr > δ34SCAS) in the terminal Proterozoic Nama group, southern Namibia: A consequence of low seawater sulfate at the dawn of animal life. *Geology* **37**, 743–746 (2009).
66. T. J. Algeo, G. M. Luo, H. Y. Song, T. W. Lyons, D. E. Canfield, Reconstruction of secular variation in seawater sulfate concentrations. *Biogeosciences* **12**, 2131–2151 (2015).
67. G. M. Cox *et al*., Neoproterozoic iron formation: An evaluation of its temporal, environmental and tectonic significance. *Chem. Geol.* **362**, 232–249 (2013).
68. M. A. Lechte, M. W. Wallace, A. S. Hood, N. Planavsky, Cryogenian iron formations in the glaciogenic Kingston Peak Formation, California. *Precambrian Res.* **310**, 443–462 (2018).
69. R. Guilbaud, S. W. Poulton, N. J. Butterfield, M. Zhu, G. A. Shields-Zhou, A global transition to ferruginous conditions in the early Neoproterozoic oceans. *Nat. Geosci.* **8**, 466–470 (2015).
70. A. V. S. Hood, M. W. Wallace, Marine cements reveal the structure of an anoxic, ferruginous Neoproterozoic ocean. *J. Geol. Soc. London* **171**, 741–744 (2014).
71. D. E. Canfield *et al*., Ferruginous conditions dominated later neoproterozoic deep-water chemistry. *Science* **321**, 949–952 (2008).
72. S. W. Poulton, D. E. Canfield, Ferruginous conditions: A dominant feature of the ocean through Earth's history. *Elements* **7**, 107–112 (2011).
73. Y. Hebting *et al*., Biomarker evidence for a major preservation pathway of sedimentary organic carbon. *Science* **312**, 1627–1631 (2006).
74. M. E. L. Kohnen, J. S. Sinninghe Damsté, H. L. ten Haven, J. W. de Leeuw, Early incorporation of polysulphides in sedimentary organic matter. *Nature* **341**, 640 (1989).
75. D. Bryant *et al*., "Comparative and functional genomics of anoxygenic green bacteria from the taxa Chlorobi, Chloroflexi, and Acidobacteria" in *Functional Genomics and Evolution of Photosynthetic Systems*, R. Burnap, W. Vermaas, Eds. (Springer, 2012), Vol. 33, pp. 47–102.
76. S. Heising, L. Richter, W. Ludwig, B. Schink, Chlorobium ferrooxidans sp. nov., a phototrophic green sulfur bacterium that oxidizes ferrous iron in coculture with a "Geospirillum" sp. strain. *Arch. Microbiol.* **172**, 116–124 (1999).
77. X. A. Walter *et al*., Phototrophic Fe(II)-oxidation in the chemocline of a ferruginous meromictic lake. *Front. Microbiol.* **5**, 713 (2014).
78. D. A. Bryant, Z. Liu, "Green bacteria: Insights into green bacterial evolution through genomic analyses" in *Genome Evolution of Photosynthetic Bacteria*, J. T. Beatty, Ed. (Advances in Botanical Research, Elsevier, 2013), Vol. 66, pp. 99–150.
79. R. Rippka, J. Deruelles, J. B. Waterbury, M. Herdman, R. Y. Stanier, Generic assignments, strain histories and properties of pure cultures of cyanobacteria. *Microbiology* **111**, 1–61 (1979).
80. S. E. Stevens Jr., C. O. P. Patterson, J. Myers, The production of hydrogen peroxide by blue-green algae: A survey. *J. Phycol.* **9**, 427–430 (1973).
81. Y. Hoshino *et al*., Cryogenian evolution of stigmasteroid biosynthesis. *Sci. Adv.* **3**, e1700887 (2017).
82. A. J. M. Jarrett, R. Schinteie, J. M. Hope, J. J. Brocks, Micro-ablation, a new technique to remove drilling fluids and other contaminants from fragmented and fissile rock material. *Org. Geochem.* **61**, 57–65 (2013).
83. C. J. Illing *et al*., Heterogeneity of free and occluded bitumen in a natural maturity sequence from Oligocene Lake Enspel. *Geochim. Cosmochim. Acta* **245**, 240–265 (2019).
84. M. P. Koopmans, J. W. De Leeuw, J. S. Sinninghe Damsté, Novel cyclised and aromatised diagenetic products of β-carotene in the Green River Shale. *Org. Geochem.* **26**, 451–466 (1997).